Interplay between mutational pathway and spatial drug distribution controls time to evolution of drug resistance (supplemental material)

Philip Greulich*, Bartłomiej Waclaw,* and Rosalind J. Allen

I. PARAMETERS USED IN OUR MODEL

Growth rate. We assume that the growth rate of genotype m depends on the drug concentration c as $\phi_m(c) = f(c/c_m^{\rm mic})$, where $c_m^{\rm mic}$ denotes the minimal inhibitory concentration (MIC; the drug concentration at which genotype m ceases to grow), and $f(x)$ is a function which is the same for all genotypes and reads

$$f(x) = \max\{0, 1 - x^\kappa\}. \tag{I.1}$$

$\kappa > 0$ being some positive constant. The form (I.1) is chosen to approximate the sigmoidal function obtained by fitting to experimental data (c.f. Eqs. (1) and (2) in Ref. [1])

$$f(x) = 1 - 2\frac{x^\kappa}{1+x^\kappa}, \tag{I.2}$$

where $x^\kappa/(1+x^\kappa)$ is the Hill function. The Hill coefficient κ has been determined experimentally to be in the range $\kappa = 0.5 \ldots 2.5$ for different antibiotics [1]. In our paper we assume an integer value $\kappa = 2$ which is consistent with experimental data and also makes the numerical evaluation of Eq. (I.1) highly efficient in our simulations.

Death rate d. The role of death in our model is to ensure that the population continues to turn over in the steady state. In the absence of death, a static state would be reached in which the environment would be completely filled by bacteria, i.e., $N_i = K$ for every compartment i, no reproduction would occur and thus no further evolution would be possible. Although we try to avoid this in our simulations, such a static state is not necessarily unrealistic in a laboratory setting where, for example, a bacterial colony grows until the available nutrients and space are exhausted. In the natural environment, however, cells are likely to be removed at a non-zero rate, either by being washed out by flow (e.g. for gut bacteria), by being killed by the immune system (or by phage in the case of bacteria), or by being poisoned by their own waste products. In our simulations, we set the death rate $d = 0.1$; this is large enough to provide significant population turnover (and hence evolution), but small enough to keep the concentration of bacteria close to the maximal environmental capacity K.

Mechanism of drug action It is important to note that in our model, it is the growth rate rather than the death rate which is dependent on the drug concentration – the drug does not kill the cells directly but simply prevents their reproduction. Our results are therefore valid for cytostatic, rather than cytocidal, drugs. We have, however, checked that most of the conclusions of the paper are valid also for cytocidal drugs, for which the death rate increases with the drug concentration.

Number of habitats L and carrying capacity K. We aimed to choose values of L and K in as close correspondance as possible with the recent experiments of Zhang *et al.* [3], while remaining within the limits of computational feasibility. In Zhang *et al.*'s experiments, *Escherichia coli* bacteria evolve in a microfluidic device containing many microhabitats, exposed to an antibiotic gradient [3]. In this experiment, 1200 hexagonal wells are arranged into a 2d hexagonal lattice. Each well has a volume of about $10^6\mu$m^3 and is connected to six other wells by narrow channels of length 200μm and having a cross-section of 100μm^2. Assuming that the maximal density of bacteria growing on LB broth used in this experiment is $\rho \approx 10^9$ cells/ml, we conclude that each well has a carrying capacity of about 1000 cells. In our model, for conceptual and computational simplicity, we use instead a linear array of microhabitats, with the number of habitats L between 100 and 500, and, in the interests of computational speed, we use a carrying capacity $K = 100$ which is lower by about one order of magnitude than in the experiments of Zhang *et al.*.

Migration rate. We assume that the rate of migration $b = 0.1$ per cell is small in comparison to the maximal growth rate $\phi = 1$. As well as simplifying our calculations of the fixation probability (since each compartment can be treated as isolated), this also represents the case in which compartments are connected by narrow channels, as in the microfluidic experiments of Zhang *et al.* [3]. The characteristic timescale of migration $t_{\rm migr}$ in such an experiment can be deduced as follows. Assuming that each microhabitat has linear size l and is connected to its neighbouring microhabitat by a channel of width w (we neglect the length of the channel), $t_{\rm migr} \sim (l/w) \times l^2/D$, where D is the effective cell diffusion rate. In the experiments of Ref. [3] we estimate that $l = 200\mu$m, $w = 10\mu$m and $D = 100$–1000μm^2/s (typical values for *E. coli*), so that $t_{\rm migr} \sim 10^3$–10^4s. Since the typical reproduction time of *E. coli* in LB medium is $t_{\rm rep} \sim 10^3$s, we obtain $b = t_{\rm rep}/t_{\rm migr} = 0.1$–$1$.

Mutation probability μ. We assume that the probability μ to mutate into genotypes $m \pm 1$ during replication is small enough so that at most one mutant arises in a completely filled environment, per cell generation: $\mu KL \leq 1$.

*Equal contribution

For wild-type strains of the bacterium *E. coli*, the mutation probability is typically $\mu \approx 10^{-9}$ per cell per generation REFERENCE?, so that this condition would imply a total population KL of $< 10^9$ cells. In our simulations the maximal population KL lies in the range 10^4 to 10^5 cells. To ensure that our simulations are computationally feasible, while remaining consistent with the condition $\mu KL \leq 1$, we choose mutation rates in the range $\mu = 5 \times 10^{-6}$ to $\mu = 10^{-4}$.

Length of mutational pathways and MIC values. Our choices of $M = 6$ (corresponding to 5 mutated genotypes along the pathway to resistance) and of MIC values $c_m^{\rm mic} = 4^m$ (which, for $M = 6$, spans three orders of magnitude between wild-type and full resistance) are inspired by two sources. In Ref. [2], Weinreich *et al* show that 5 different single-nucleotide substitutions (SNPs) increase the resistance of *E. coli* to the antibiotic cefotaxime by a factor of 10^5, from $c^{\rm mic} = 0.063\mu$g/ml to 4100μg/ml (~ 4 orders of magnitude), and that the evolution of this resistance follows typically only one or two pathways in genotype space. Furthermore, in Ref. [3], Zhang *et al* found four SNPs in evolved strains for which resistance to the antibiotic ciprofloxacin was increased by a factor ~ 200 (~ 2 orders of magnitude).

II. MONTE CARLO SIMULATIONS

Our simulations use a simple but computationally efficient algorithm which chooses an individual cell at random, calculates transition rates for each of the possible events that may happen to that cell (i.e. migration, death and replication, possibly accompanied by mutation), and executes one of these processes with probability proportional to its associated transition rate. More specifically each step of the simulation consists of the following:

- draw a random number $i = 1, \ldots, N_{\rm tot}$ in order to choose a cell from the $N_{\rm tot}$ cells in the system. We denote by j and m the position and the genotype, respectively, of this cell.
- calculate the rates $R_{\rm migr} = b$, $R_{\rm death} = d$ and $R_{\rm growth} = \phi_m(c_j)(1 - N_j/K)$, at which the cell may migrate to a neighboring microhabitat, die or replicate.
- draw a random number $r \in [0 \ldots R_{\rm max})$, where $R_{\rm max}$ is greater than or equal to the maximal value of $R_{\rm migr} + R_{\rm death} + R_{\rm growth}$ which may be ever encountered in the simulation. In our simulations we use $R_{\rm max} = 1.2$.
- execute migration if $r < R_{\rm migr}$, death if $R_{\rm migr} \leq r < R_{\rm migr} + R_{\rm death}$ and replication if $R_{\rm migr} + R_{\rm death} \leq r < R_{\rm migr} + R_{\rm death} + R_{\rm growth}$ (for replication see below). In the case that $r \geq R_{\rm migr} + R_{\rm death} + R_{\rm growth}$, execute none of these processes.
- if executing a replication step, draw an additional random number $s \in [0 \ldots 1)$. If $s < \mu/2$, add to the system one new cell of genotype $m + 1$. If $\mu/2 < s < \mu$, instead add a new cell of genotype $m - 1$. Otherwise, add a new cell of genotype m.
- update the simulation time $t \to t + \Delta t$, where $\Delta t = 1/(N_{\rm tot} R_{\rm max})$.

This method works much faster for our model than the standard Gillespie algorithm [4]. This is because few calculations are required to iterate each step and, since the total rate $0.2 \leq R_{\rm growth} + R_{\rm migr} + R_{\rm death} \leq 1.2$ is bounded both from above and below, the fraction of steps in which an event happens (i.e. we obtain $r < R_{\rm migr} + R_{\rm death} + R_{\rm growth}$) is high (greater than 25%). This algorithm exactly simulates our stochastic model, the only exception being that distribution of times between events is not a continuous exponential function (as in the Gillespie algorithm) but is discretized (in steps of $\Delta t = 1/(N_{\rm tot} R_{\rm max})$), with the correct mean value. This is not important on the timescales considered in this work, which are very long compared to the time between simulation events.

III. TIME TO FIXATION IN THE UNIFORM ENVIRONMENT

Here, we discuss the calculation of the time to fixation (which we denote $T_{\rm fix}$) of genotype $m + 1$ in the uniform environment, in the case where each genotype along the pathway to resistance is fitter than the preceding one (MIC increases with m). For notational simplicity, in what follows we replace the genotype labels m and $m+1$ with A and B respectively.

Since the drug is uniformly distributed, the fitness difference $\phi_B - \phi_A > 0$ between genotypes A and B is everywhere the same. As for the heterogeneous environment (see main text), we assume strong selection – i.e. $\phi_B - \phi_A \gg 1/K$. We suppose that the system is initially populated by genotype A; the steady-state population $N_A^* = K(1 - d/\phi_A)$ is the same in each microhabitat. We assume that genotype B takes over the population in two stages: it first emerges and fixes locally in one of the L microhabitats, and then spreads out from this microhabitat to take over the entire population. The timescale for local emergence and fixation in a microhabitat anywhere in the system is given by $T_{\rm loc} = [(\mu d/2)(N_A^* L)(\phi_B - \phi_A)/\phi_B]^{-1}$ (this is analogous to Eq.(2) from the main text, assuming uniformity over the microhabitat).

To compute the timescale over which genotype B then spreads as an "invasion wave" across the whole system, we resort to a continuous space approximation (as in Eq.(1) of the main text), modelling the system by two coupled

Fisher-KPP equations:

$$\partial_t N_A = \frac{b}{2}\partial_{xx} N_A + \phi_A N_A \left(1 - \frac{N_{\rm tot}}{K}\right) - dN_A, \quad \text{(III.1)}$$

$$\partial_t N_B = \frac{b}{2}\partial_{xx} N_B + \phi_B N_B \left(1 - \frac{N_{\rm tot}}{K}\right) - dN_B, \quad \text{(III.2)}$$

where $N_{\rm tot} = N_A + N_B$. To calculate the velocity with which genotype B invades the population of genotype A, we proceed along standard lines [6]; we insert an asymptotic solution $N_B(x,t) = \exp(-\lambda(x - vt))$ (note that we assume genotype B invades from the left) and the steady-state solution for $N_A(x,t) = N_A^*$ into Eq. (III.2), and linearise the resulting equation. This leads to the relation

$$\frac{b}{2}\lambda^2 - \lambda v + d\left(\frac{\phi_B}{\phi_A} - 1\right) = 0. \quad \text{(III.3)}$$

The smallest value of v for which Eq. (III.3) has a real, positive solution $\lambda > 0$ is

$$v = \left(\frac{2bd(\phi_B - \phi_A)}{\phi_A}\right)^{1/2}. \quad \text{(III.4)}$$

Eq. (III.4) gives the velocity of the invasion wave of genotype B. This allows us to determine the timescale $T_{\rm prop} = L/v$ over which the better adapted genotype B spreads to take over the entire population.

The time $T_{\rm fix}$ for genotype B to fix in the entire population depends critically on the relative magnitudes of $T_{\rm loc}$ and $T_{\rm prop}$. If the invasion wave propagates rapidly ($T_{\rm prop} \ll T_{\rm loc}$), $T_{\rm loc}$ determines the time to global fixation and we have

$$T_{\rm fix} \propto (\phi_B - \phi_A)^{-1}. \quad \text{(III.5)}$$

In this case the fitter genotype B, once established locally, spreads quickly to take over the population; there is then a waiting time before an even fitter mutant has a chance to arise and in turn invade the population. Evolution of resistance thus proceeds in a sequence of distinct steps, each corresponding to the emergence and spread of a separate mutant. The condition $T_{\rm prop} \ll T_{\rm loc}$ places a limit on the mutation rate for this scenario to hold:

$$\mu \ll \mu_0 = \frac{\phi_B}{L^2 N_A^*}\left(\frac{8b}{d\phi_A(\phi_B - \phi_A)}\right)^{1/2}. \quad \text{(III.6)}$$

If, on the other hand, the time of propagation of the invasion wave is equal to or longer than the typical time of local fixation, a different scenario holds. This is relevant for higher mutation rates $\mu \gg \mu_0$ (but still assuming a low mutation probability per generation $\mu KL \leq 1$). In this case, new, fitter mutants can arise and fix locally before the preceding mutant has taken over the entire population. This produces a population with a "shell-like" structure: genotype $m+1$ ($= B$) emerges inside the invasion wave of genotype m ($= A$) as it spreads in both directions; this wave of genotype m is itself enclosed within another spreading wave of genotype $m-1$, etc. To compute the time to fixation for genotype $m+1$ ($= B$) within the spreading wave of genotype m ($= A$), we need to take account of the fact that the population size of genotype A increases in time as its wave spreads: the total population grows as $N_A^* v_A t$, where v_A is the velocity at which genotype $A = m$ spreads in the population of the preceding, less fit, genotype $m-1$ (or in an empty environment if $m = 1$). The rate at which mutants of genotype $B = m+1$ fix is then given by $\Omega(t) = (\mu d/2)(N_A^* v_A t)(\phi_B - \phi_A)/\phi_B$ (c.f. Eq. (2) in the main text and the derivation of $T_{\rm loc}$ earlier in this section; the term $(\phi_B - \phi_A)/\phi_B$ is the fixation probability of genotype B in the population of A). Since $\Omega(t) \propto t$ increases with time, the fixation of genotype B cannot be treated as a Poisson process; the distribution of times to fixation is not exponential but is rather given by

$$P(t) = \Omega(t) e^{-\int_0^t \Omega(t')dt'} = \omega t e^{-\omega t^2/2}, \quad \text{(III.7)}$$

where we have introduced $\omega = (\mu d/2) N_A^* v_A (\phi_B - \phi_A)/\phi_B$. The average time to fixation of B is then

$$T_{\rm fix} = \int_0^\infty P(t) t {\rm d}t = \sqrt{2\pi/\omega} \propto v_A^{-1/2} (\phi_B - \phi_A)^{-1/2}. \quad \text{(III.8)}$$

To summarize, for the low mutation rates $\mu < (KL)^{-1}$ considered in this work, the time $T_{\rm fix}$ for genotype $m+1$ to take over the population of genotype m scales as $T_{\rm fix} \propto (\phi_{m+1} - \phi_m)^{-\gamma}$, where the value of the exponent γ depends on the mutation rate. For ultra-low mutation rates $\mu < \mu_0$ (see Eq. (III.6)), $\gamma = 1$, while for more frequent mutations (for which $\mu_0 < \mu < (KL)^{-1}$), $\gamma = 1/2$. Since in our model the fitness difference $\phi_{m+1} - \phi_m$ becomes smaller as m grows, $T_{\rm fix}$ increases with m and hence, as long as the strong selection approximation still holds (see main text), the time to evolve better adapted mutants increases with the number of mutations.

IV. FIXATION TIME FOR NON-UNIFORM DRUG CONCENTRATION, FOR SPECIFIC MODEL ASSUMPTIONS

For the specific choices of drug concentration profile and MIC values used in our model, we can calculate explicitly the time $T_{m+1}^{\rm mut}$ for genotype $m+1$ to establish in the quasi-stationary population of genotype m, in the case of non-uniform drug concentration. This requires us to evaluate the integral of Eq. (2) in the main text. In our simulations, we assume that the drug concentration increases exponentially with x as $c(x) = e^{\alpha x} - 1$, the MICs increase exponentially with m as $c_m^{\rm mic} = 4^{m-1}$, and the growth rate is a function of $c/c_m^{\rm mic}$, i.e. $\phi_m = f(c/c_m^{mic})$.

Substituting into Eq. (2) of the main text the result $N_m^*(x) = K[1 - d/\phi_m(c(x))]$ (from the main text) and $\phi_m(c) = f(c/c_m^{\rm mic})$, noting that $\phi_{m+1}(c) \approx 1$ for $c < c_m^{\rm mic}$ and changing the integration variable to $z = c(x)/c_m^{\rm mic} =$

$(e^{\alpha x/L}-1)/4^{m-1}$, gives

$$T^{\rm mut}_{m+1} \approx \frac{2\alpha}{\mu d K L}\left[\int_{z(x^*_{m-1})}^{z(x^*_m)} dz \frac{(f(z)-d)(1-f(z))}{(z+4^{m-1})f(z)}\right]^{-1}. \quad \text{(IV.1)}$$

Here, $z(x^*_m) = (e^{\alpha x^*_m}-1)/4^{m-1}$. The positions x^*_m of the stationary fronts are given by $x^*_m = (1/\alpha)\ln(c^{\rm mic}_m\sqrt{(1-d)}+1)$ (see main text), which, for our choice of $c^{\rm mic}_m$ and for large m, becomes $x^*_m \approx (1/\alpha)(m-1)\ln(4\sqrt{1-d})$.

The limits of the integral in Eq. (IV.1) are therefore $z(x^*_m) = \sqrt{1-d}$ and $z(x^*_{m-1}) \approx \sqrt{1-d}/4$. Inserting these limits, we see that $T^{\rm mut}_{m+1}$ becomes independent of m for $m \gg 1$:

$$T^{\rm mut} := T^{\rm mut}_{m+1} \approx \frac{2\alpha}{\mu d K L}\left[\int_{\sqrt{1-d}/4}^{\sqrt{1-d}} dz \frac{(f(z)-d)(1-f(z))}{z f(z)}\right]^{-1} \quad \text{(IV.2)}$$

This result holds independently of the details of the growth rate (fitness) function ϕ_m, as long as ϕ_m is a function of $c/c^{\rm mic}_m$.

For the specific choice of $\phi_m(c/c^{\rm mic}_m)$ used in our simulations (see main text), we have $\phi_m(z) = 1-z^2$, and the integral reads $\int_{\sqrt{1-d}/4}^{\sqrt{1-d}} dz\, z(1-d-z^2)/(1-z^2)$; this yields

$$T^{\rm mut} = \frac{\alpha}{\mu d K L}\left((1-d)\frac{15}{16} + d\ln(16d/15)\right) \quad \text{(IV.3)}$$

$$\approx \frac{\alpha}{\mu d K L}(1-d+d\ln d) \quad \text{(IV.4)}$$

Since $T^{\rm mut}$ is independent of m, the average time to resistance $\bar\tau$, as specified in Eq. (3) of the main text, scales linearly with M as long as the expansion of the population is not limited by the boundaries of the system. If the population reaches a constraining boundary before full resistance has emerged, subsequent mutants will have only a very small fitness advantage: the resulting neutral competition greatly slows the evolution of full resistance.

V. SCALING WITH PATHWAY LENGTH, FOR FIXED MAXIMAL FITNESS

In Fig. 3 of the main text, we present results for the scaling of the time to resistance with the length M of the mutational pathway. Those results were obtained assuming, as in the rest of the main text, that the MIC of genotype m is given by $c^{\rm mic}_m = 4^{m-1}$. In that scenario, as the pathway length increases, the MIC of the most resistant genotype increases as $c^{\rm mic}_M = 4^{M-1}$. Here, we investigate the aternative case, where we vary the number of intermediate genotypes, keeping fixed the fitness of the most resistant genotype: i.e. change M keeping $c^{\rm mic}_M$ fixed. We show that the main results of Fig. 3 in the main text remain valid in this alternative scenario.

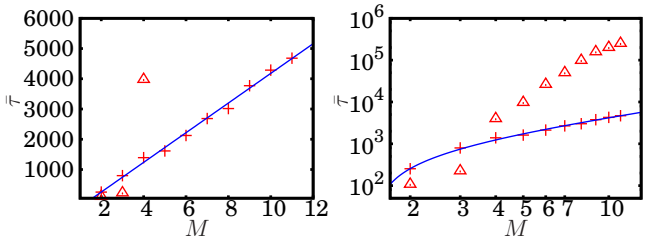

Figure V.1. Average time to full resistance $\bar\tau$ in dependence on the mutational pathway length M, determined numerically for fixed maximum resistance $c^{\rm mic}_M = 4^5$, plotted on a linear (left) and log-log scale (right). Compared are homogeneous (triangles) and heterogeneous ($\alpha = 0.07$, pluses) drug distribution. The blue line shows a linear fit. We have in both cases $L = 100, K = 100, \mu = 10^{-4}$. In fact, the time τ grows linearly for heterogeneous drug distribution as predicted by the theory.

Fig. V.1 shows the results of simulations in which we fix $c^{mic}_1 = 1$ and $c^{mic}_M = 4^5$ and set the resistance of intermediate genotypes according to $c^{\rm mic}_m = 4^{5(m-1)/(M-1)}$. Plotting the average time to resistance as a function of the length M of the mutational pathway, we obtain qualitatively similar behaviour to that shown in Fig. 3 of the main text: for short pathways, resistance evolves faster in the case of uniform drug but for longer pathways, evolution is much faster in the non-uniform case.

From a theoretical point of view, Eq. (3) of the main text remains valid (for the non-uniform case); as in the main text, successive population waves are of the same shape but now their positions x^*_m are no longer equidistant. The contributions $T^{\rm wave}_m$ are then different for different m, but the sum

$$\sum_{m=1}^{M-1} T^{\rm wave}_m = \sum_{m=1}^{M-1}(x^*_m - x^*_{m-1})/v = x^*_M/v \quad \text{(V.1)}$$

is independent of M since fixed c^{mic}_M implies fixed x^*_M. The contributions $T^{\rm mut}_m$ are also in principle different for different m. However, because the evolution of the next genotype happens almost exclusively close to the leading edge of the stationary front, in practice $T^{\rm mut}_m$ remains independent of m. We therefore expect linear scaling of $\bar\tau$ with M, as is indeed apparent in Fig. V.1 for the non-uniform drug concentration.

[1] R. R. Regoes, C. Wiuff, R. M. Zappala, K. N. Garner, F. Baquero, and B. R. Levin, Antimicrob. Agents Chemother. **48**, 3670 (2004).

[2] D. M. Weinreich, N. F. Delaney, M. A. DePristo, and D. L. Hartl, Science **312** 111 (2006).
[3] Q. Zhang et al., Science **333** 1764 (2011).
[4] D. T. Gillespie, J. Phys. Chem. **81** 2340 (1977).
[5] M. A. Nowak, *Evolutionary dynamics. Exploring the Equations of Life*, Belknap Press (2006).
[6] J. D. Murray, *Mathematical Biology*, 3rd edition, Vol.1, Springer (2002).